

Tubular Assemblies of N-doped Carbon Nanotubes Loaded with NiFe Alloy Nanoparticles as Efficient Bifunctional Catalysts for Rechargeable Zinc-air Batteries

Supporting Information

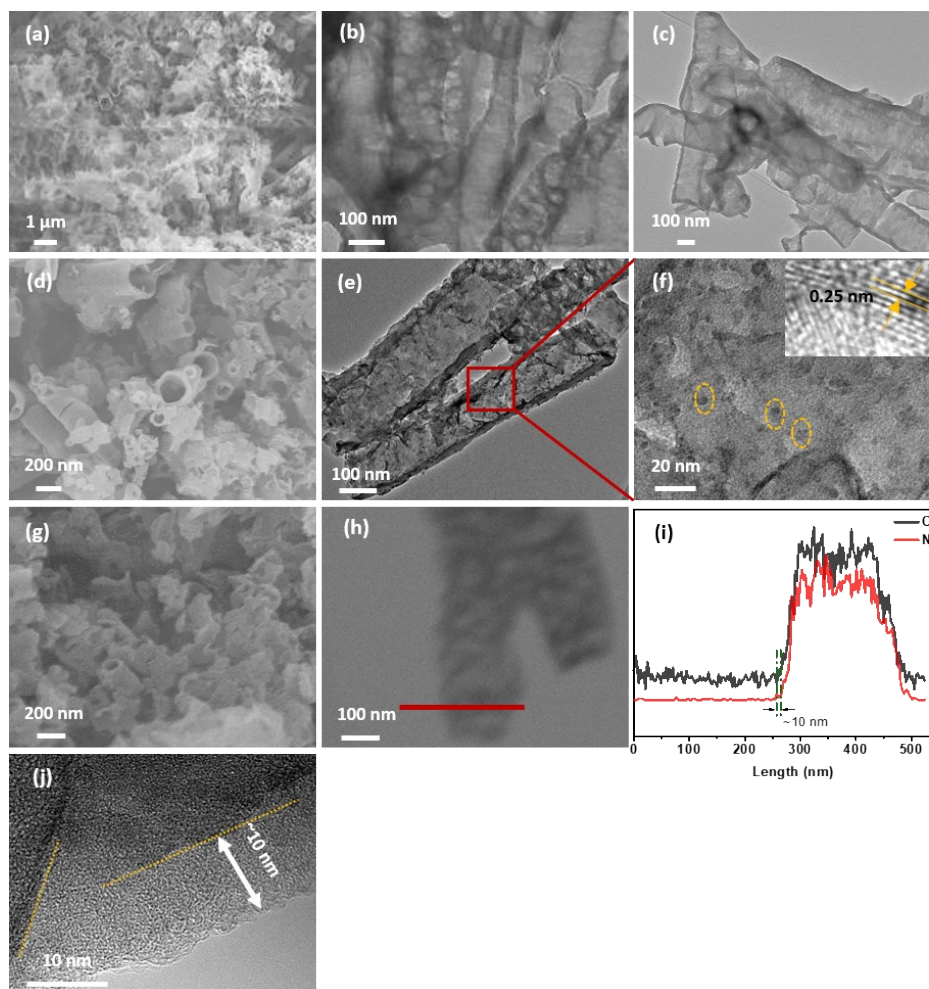


Fig. S1 SEM images for (a) $g\text{-C}_3\text{N}_4$ nanotubes, (d) NiFe-LDH/ $g\text{-C}_3\text{N}_4$, and (g) NiFe-LDH/ $g\text{-C}_3\text{N}_4$ @Glu. (b, c) Low-magnification TEM images for $g\text{-C}_3\text{N}_4$ nanotubes. (e, f) High-magnification TEM images for NiFe-LDH/ $g\text{-C}_3\text{N}_4$. Linear scanning data (h, i) and high-magnification TEM image (j) for NiFe-LDH/ $g\text{-C}_3\text{N}_4$ @Glu.

Fig. S1e and f show that NiFe-LDH nanocrystals (~ 5 nm) were uniformly distributed over the tubular $g\text{-C}_3\text{N}_4$. The lattice spacing of 0.25 nm in Fig. S1f, corresponding to the (012) facet of NiFe-LDH, further confirms the formation of NiFe-LDH and is consistent with those in the literatures.^{1, 2} The linear scanning data shown in Fig. S1h and i, and high-magnification TEM image in Fig. S1j confirm that the thickness of the coating layer was about 10 nm. The layer (Fig. S1j) was dominated by curved carbon fringes and lack of long-range ordering carbon structure, typical characteristics of amorphous carbon.³

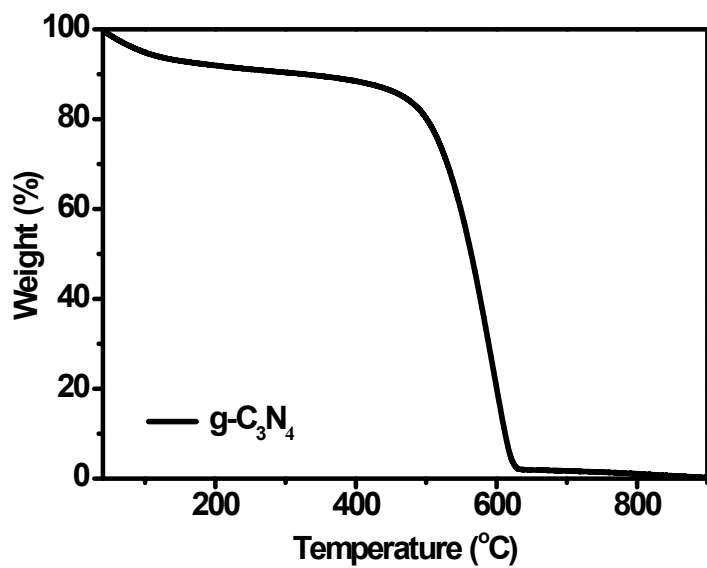


Fig. S2 TGA for g-C₃N₄ nanotubes in a N₂ atmosphere. The heating rate was 5 °C min⁻¹.

Many literatures reported that g-C₃N₄ could decompose completely in inert atmosphere at high temperature⁴⁻⁶ and release CN gases (e.g. C₂N₂⁺, C₃N₂⁺, C₃N₃⁺)⁷, which provide abundant source of C and N.

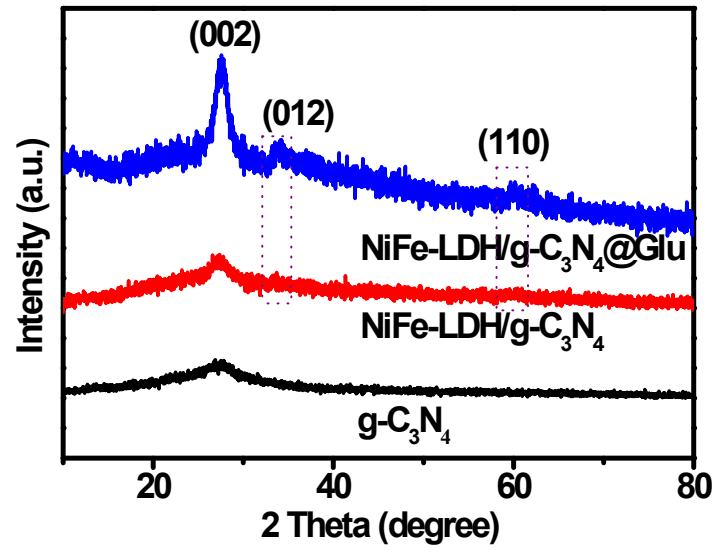


Fig. S3 XRD patterns for $g\text{-C}_3\text{N}_4$, NiFe-LDH/ $g\text{-C}_3\text{N}_4$, and NiFe-LDH/ $g\text{-C}_3\text{N}_4\text{@Glu}$.

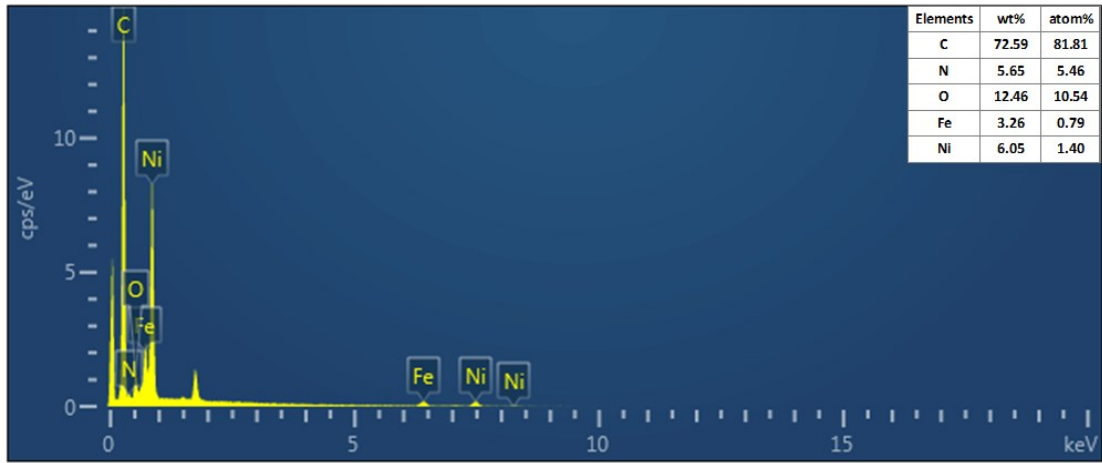


Fig. S4 EDS spectrum for TA-NiFe@NCNT.

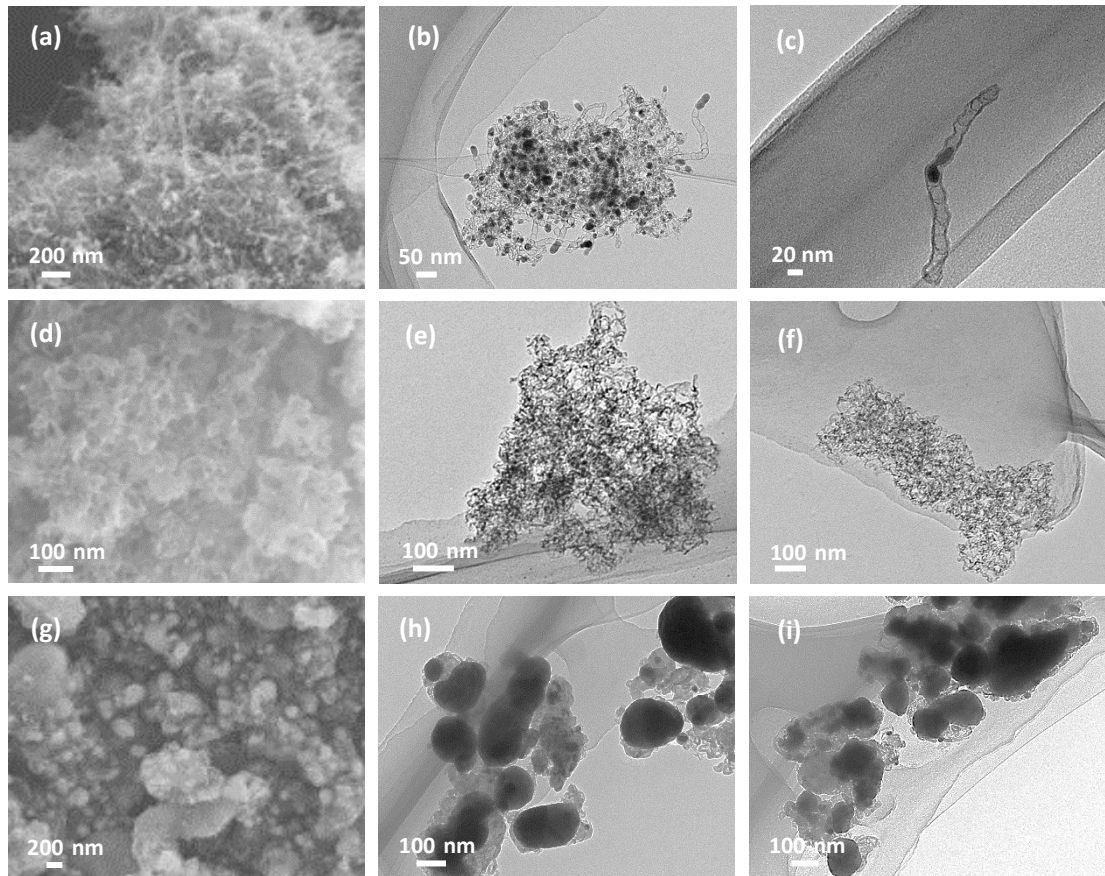


Fig. S5 SEM images for (a) TA-NiFe@NCNT, (d) TA-NC, and (g) NiFe/C. TEM images for (b, c) TA-NiFe/NCNT, (e, f) TA-NC, and (h, i) NiFe/C.

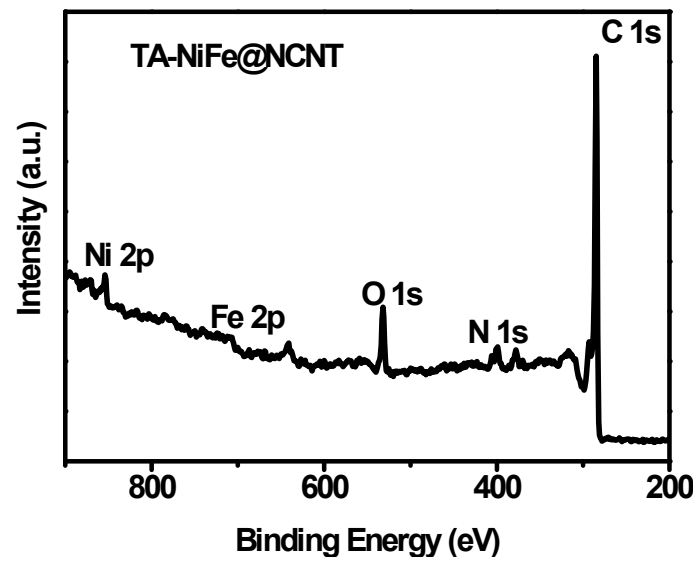


Fig. S6 XPS survey spectrum for TA-NiFe@NCNT.

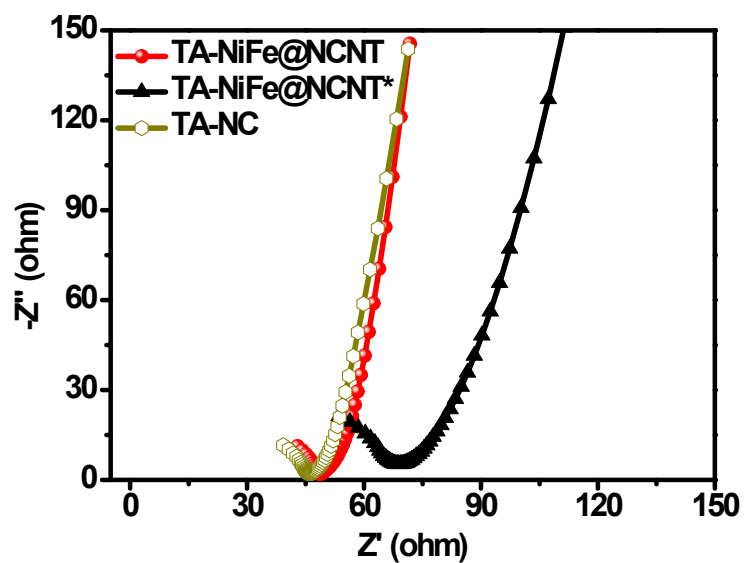


Fig. S7 Nyquist plots of the impedance data for TA-NiFe@NCNT, TA-NiFe@NCNT*, and TA-NC.

Nyquist plots were obtained from electrochemical impedance spectroscopy (EIS) measurements. EIS data were measured over the frequency range 0.1 Hz to 10 kHz with an AC amplitude of 10 mV at the open-circuit voltage.

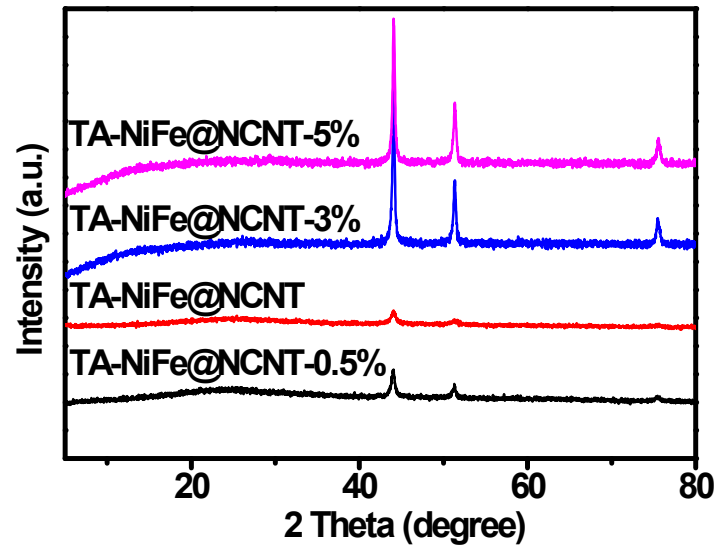


Fig. S8 XRD patterns for TA-NiFe@NCNT-0.5%, TA-NiFe@NCNT, TA-NiFe@NCNT-3%, and TA-NiFe@NCNT-5%.

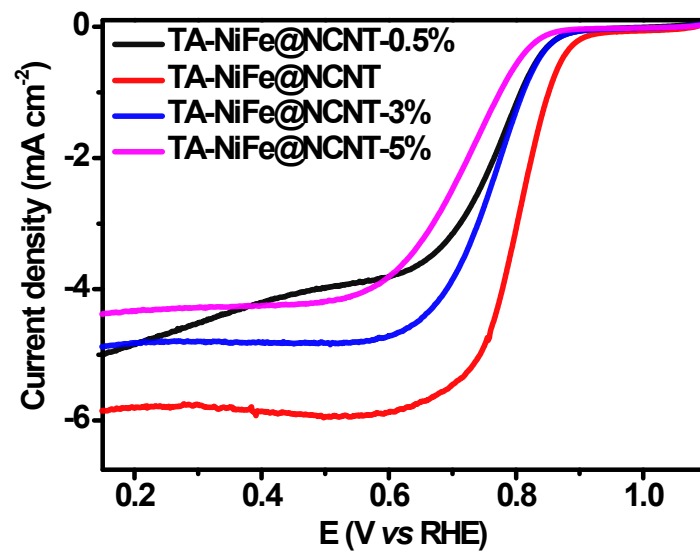


Fig. S9 ORR LSV curves for TA-NiFe@NCNT-0.5%, TA-NiFe@NCNT, TA-NiFe@NCNT-3%, and TA-NiFe@NCNT-5% at a rotation speed of 1600 rpm and a scan rate of 10 mV s⁻¹.

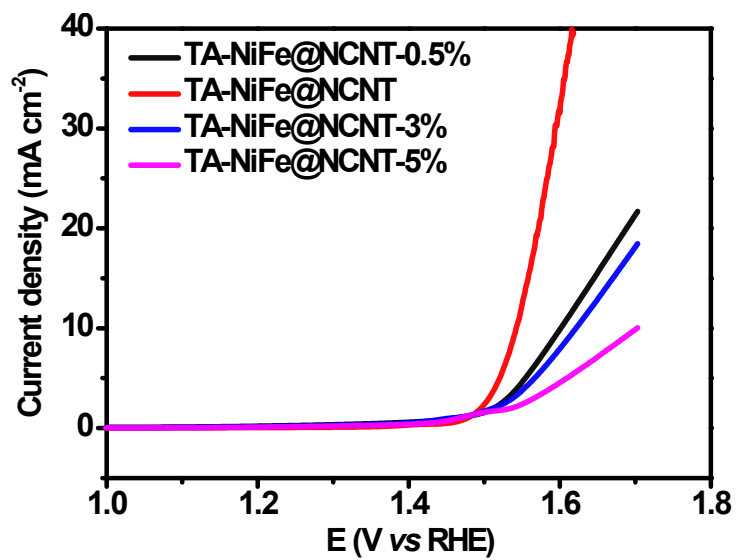


Fig. S10 OER LSV curves for TA-NiFe@NCNT-0.5%, TA-NiFe@NCNT, TA-NiFe@NCNT-3%, and TA-NiFe@NCNT-5% at a rotation speed of 1600 rpm and a scan rate of 5 mV s⁻¹ (after 95%-IR correction).

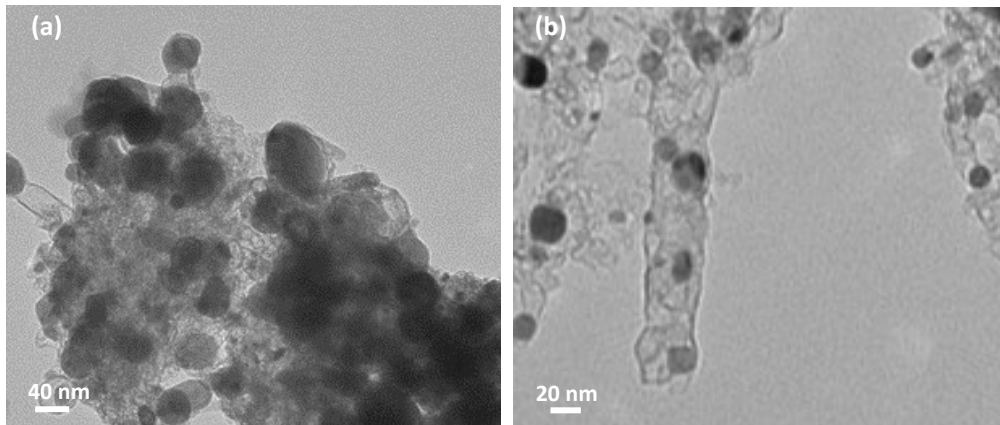


Fig. S11 TEM images for (a) TA-NiFe@NCNT-5%, and (b) TA-NiFe@NCNT-0.5%.

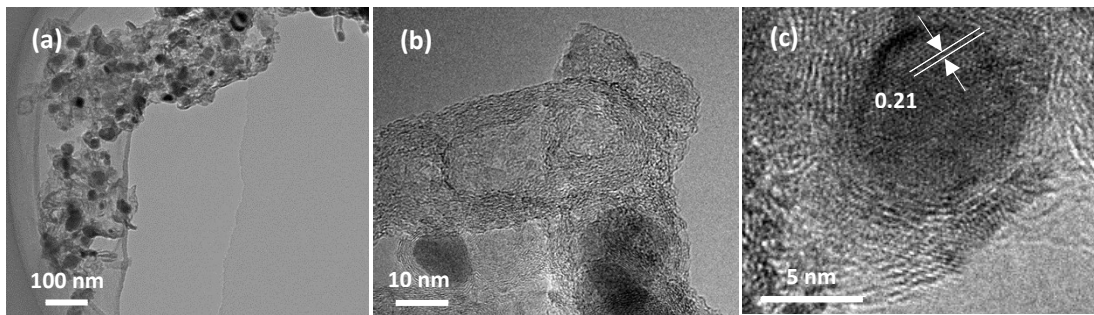


Fig. S12 (a-c) TEM images of TA-NiFe@NCNT after 170 h of charge and discharge cycling at a current density of 25 mA cm^{-2} .

Table S1 Comparison of the ORR and OER activities of TA-NiFe@NCNT with other reported bifunctional catalysts in 0.1 M KOH electrolyte.

Catalysts	E_{OERj10}	$E_{\text{ORR1/2}}$	$\Delta E = E_{\text{OERj10}} - E_{\text{ORR1/2}}$	Reference
TA-NiFe@NCNT	1.54 V	0.81 V	0.73 V	This work
TA-NiFe@NCNT*	1.57 V	0.78 V	0.79 V	This work
Pt/C+IrO ₂	1.63 V	0.82 V	0.81 V	This work
NiFe/N-CNT	1.52 V	0.75 V	0.77 V	8
m-NiFe/CNx	1.59 V	0.76 V	0.83 V	9
NiFe@NBCNT	---	0.83 V	---	4
Ni ₃ Fe/N-C sheets	1.60 V	0.78 V	0.82 V	10
S, N-Fe/N/C-CNT	1.60 V	0.85 V	0.75 V	11
N-GCNT/FeCo-3	1.73 V	0.92 V	0.81 V	12
CoFe/@NCNTs	1.68 V	0.84 V	0.84 V	13
meso/micro-FeCo-Nx-CN-30	1.60 V	0.886 V	0.714 V	14
NiFe-LDH/Co, N-CNF	1.54 V	0.79 V	0.75 V	15
NCNT/CoONiO-NiCo	1.50 V	0.78 V	0.72 V	16
0.1-Co-NHCs	1.65 V	0.81 V	0.84 V	17
Fe@C-NG/NCNTs	1.68 V	0.84 V	0.84 V	18

Table S2 Comparison of the rechargeable zinc-air batteries performance between TA-NiFe@NCNT, a mixture of Pt/C and IrO₂, and other bifunctional catalysts.

Catalysts	Cycling current density (mA cm ⁻²)	Cycling time	Charge and discharge potential gap	Reference
TA-NiFe@NCNT	25	170 h	0.92 V	This work
Pt/C+IrO ₂	25	70 h	0.94 V	This work
NiFe/N-CNT	5	100 h	0.75 V	8
NiFe@NBCNT	10	120 h	~0.8 V	4
Ni ₃ Fe/N-C sheets	10	420 h	0.78 V	10
N-GCNT/FeCo-3	20	9 h	0.26 V	12
meso/micro-FeCo-Nx-CN-30	10	20 h	0.91 V	14
NiFe-LDH/Co, N-CNF	25	80 h	1 V	15
NCNT/CoONiO-NiCo	20	17 h	0.86 V	16
0.1-Co-NHCs	10	50 h	0.84 V	17
Fe@C-NG/NCNTs	10	99 h	0.89 V	18

Reference

- 1 Q. Wang, L. Shang, R. Shi, X. Zhang, Y. F. Zhao, G. I. N. Waterhouse, L.-Z. Wu, C.-H. Tung and T. R. Zhang, *Adv. Energy Mater.*, 2017, **7**, 1700467.
- 2 C. Tang, H.-S. Wang, H.-F. Wang, Q. Zhang, G.-L. Tian, J.-Q. Nie and F. Wei, *Adv. Mater.*, 2015, **27**, 4516-4522.
- 3 H. G. Zhang, H. T. Chung, D. A. Cullen, S. Wagner, U. I. Kramm, K. L. More, P. Zelenay and G. Wu, *Energy Environ. Sci.*, 2019, **12**, 2548.
- 4 D. Bin, B. Yang, C. Li, Y. Liu, X. Zhang, Y. Wang and Y. Xia, *ACS Appl. Mater. Interfaces*, 2018, **10**, 26178-26187.
- 5 C.-Y. Su, H. Cheng, W. Li, Z.-Q. Liu, N. Li, Z. F. Hou, F.-Q. Bai, H.-X. Zhang and T.-Y. Ma, *Adv. Energy Mater.*, 2017, **7**, 1602420
- 6 H. J. Yu, L. Shang, T. Bian, R. Shi, G. I. N. Waterhouse, Y. F. Zhao, C. Zhou, L.-Z. Wu, C.-H. Tung and T. R. Zhang, *Adv. Mater.*, 2016, **28**, 5080-5086.
- 7 Q. C. Wang, Y. P. Lei, Z. Y. Chen, N. Wu, Y. B. Wang, B. Wang and Y. D. Wang, *J. Mater. Chem. A*, 2018, **6**, 516-526.
- 8 H. Lei, Z. Wang, F. Yang, X. Huang, J. Liu, Y. Liang, J. Xie, M. S. Javed, X. Lu, S. Tan and W. Mai, *Nano Energy*, 2020, **68**, 104293.
- 9 S. Q. Ci, S. Mao, Y. Hou, S. M. Cui, H. Kim, R. Ren, Z. H. Wen and J. H. Chen, *J. Mater. Chem. A*, 2015, **3**, 7986-7993.
- 10 G. Fu, Z. Cui, Y. Chen, Y. Li, Y. Tang and J. B. Goodenough, *Adv. Energy Mater.*, 2017, **7**, 1601172.
- 11 P. Chen, T. Zhou, L. Xing, K. Xu, Y. Tong, H. Xie, L. Zhang, W. Yan, W. Chu, C. Wu and Y. Xie, *Angew. Chem. Int. Ed.*, 2017, **56**, 610-614.

- 12 C.-Y. Su, H. Cheng, W. Li, Z.-Q. Liu, N. Li, Z. Hou, F.-Q. Bai, H.-X. Zhang and T.-Y. Ma, *Adv. Energy Mater.*, 2017, **7**, 1602420.
- 13 P. Cai, Y. Hong, S. Ci and Z. Wen, *Nanoscale*, 2016, **8**, 20048-20055.
- 14 S. Li, C. Cheng, X. Zhao, J. Schmidt and A. Thomas, *Angew. Chem. Int. Ed.*, 2018, **57**, 1856-1862.
- 15 Q. Wang, L. Shang, R. Shi, X. Zhang, Y. Zhao, G. I. N. Waterhouse, L.-Z. Wu, C.-H. Tung and T. Zhang, *Adv. Energy Mater.*, 2017, **7**, 1700467.
- 16 X. Liu, M. Park, M. G. Kim, S. Gupta, G. Wu and J. Cho, *Angew. Chem. Int. Ed.*, 2015, **54**, 9654-9658.
- 17 S. Chen, J. Cheng, L. Ma, S. Zhou, X. Xu, C. Zhi, W. Zhang, L. Zhi and J. A. Zapien, *Nanoscale*, 2018, **10**, 10412-10419.
- 18 Q. Wang, Y. Lei, Z. Chen, N. Wu, Y. Wang, B. Wang and Y. Wang, *J. Mater. Chem. A*, 2018, **6**, 516-526.